

**This item is the archived peer-reviewed author-version of:**

Whole-genome typing and characterization of *bla<sub>VIM19</sub>*-harbouring ST383 *Klebsiella pneumoniae* by PFGE, whole-genome mapping and WGS

**Reference:**

Sabirova Julia, Xavier Basil Britto, Coppens Jasmine, Zarkotou Olympia, Lammens Christine, Janssens Lore, Burggrave Ronald, Wagner Trevor, Goossens Herman, Malhotra Surbhi.- Whole-genome typing and characterization of *bla<sub>VIM19</sub>*-harbouring ST383 *Klebsiella pneumoniae* by PFGE, whole-genome mapping and WGS

The journal of antimicrobial chemotherapy - ISSN 1460-2091 - (2016), p. 1-9

Full text (Publishers DOI): <http://dx.doi.org/doi:10.1093/JAC/DKW003>

To cite this reference: <http://hdl.handle.net/10067/1318080151162165141>

1 **Whole genome typing and characterisation of bla<sub>VIM19</sub>-harbouring**  
2 **ST383 *Klebsiella pneumoniae* by PFGE, whole genome mapping and**  
3 **sequencing**

4  
5  
6 Julia S. Sabirova<sup>a\*</sup>, Basil Britto Xavier<sup>a\*</sup>, Jasmine Coppens<sup>a</sup>, Olympia Zarkotou<sup>b</sup>, Christine  
7 Lammens<sup>a</sup>, Lore Janssens<sup>a</sup>, Ronald Burggrave<sup>c</sup>, Trevor Wagner<sup>c</sup>, Herman Goossens<sup>a</sup>, Surbhi  
8 Malhotra-Kumar<sup>a#</sup>

9 <sup>a</sup>Department of Medical Microbiology, Vaccine & Infectious Disease Institute, Universiteit Antwerpen,  
10 Antwerp, Belgium<sup>a</sup>; Department of Microbiology, Tzaneio General Hospital, Piraeus, Greece<sup>b</sup>; OpGen,  
11 Inc., Gaithersburg, Maryland, USA<sup>c</sup>.

12  
13 **Running Title:** bla<sub>VIM19</sub>-harbouring ST383 *K. pneumoniae*

14  
15 **Key words:** Whole genome sequencing, class 1 integron, integrase, *ICEPm1*, ST383, optical  
16 mapping, whole genome maps, PFGE

17 **Text word count:** 3749

18 **Synopsis word count:** 248

19  
20 \*Equal contribution authors

21 #Corresponding author mailing address: Department of Medical Microbiology, Campus Drie  
22 Eiken, University of Antwerp, S6, Universiteitsplein 1, B-2610 Wilrijk, Belgium. Phone: 32-3-  
23 265-27-52. Fax: 32-3-265-26-63. E-mail: surbhi.malhotra@uantwerpen.be

## 24 **Synopsis**

25 **Objectives:** We utilized whole-genome mapping (WGM) and WGS to characterize 12 clinical  
26 carbapenem-resistant *Klebsiella pneumoniae* (TGH1-TGH12).

27 **Methods:** All strains were screened for carbapenemase genes by PCR, and typed by MLST, PFGE  
28 (*XbaI*), and WGM (*AflIII*) (OpGen, USA). WGS (Illumina) was performed on TGH8 and TGH10.  
29 Reads were *denovo* assembled and annotated (SPAdes, RAST). Contigs were aligned directly, and  
30 after *in silico AflIII* restriction, with corresponding WGMs (MapSolver, OpGen; BioNumerics,  
31 Applied Maths).

32 **Results:** All 12 strains were ST383. Eleven of the 12 strains were carbapenem-resistant and 7  
33 harboured *bla*<sub>KPC-2</sub>, and 11, *bla*<sub>VIM-19</sub>. Varying the parameters for assigning WGM clusters showed  
34 that these were comparable to ST types, and to the 8 PFGE (sub)types ( $\geq 3$ -band difference). A  
35 95% similarity coefficient assigned all 12 WGMs to a single cluster while a 99% similarity  
36 coefficient (or  $\geq 10$  unmatched-fragment difference) assigned the 12 WGMs to 8 (sub)clusters.  
37 Based on a  $\geq 3$ -band difference between PFGE profiles, the Simpson's diversity index (SDI) of  
38 WGM (0.94, Jackknife pseudo-values CI: 0.883-0.996) and PFGE (0.93, CI: 0.828-1.000) were  
39 similar ( $p=0.649$ ). However, discriminatory power of WGM was significantly higher (SDI: 0.94,  
40 CI: 0.883-0.996) than PFGE profiles typed on a  $\geq 7$ -band difference (SDI: 0.53, CI: 0.212-0.849)  
41 ( $p=0.007$ ).

42 **Conclusions:** This study demonstrates the application of whole-genome mapping to understanding  
43 the epidemiology of hospital-associated *K. pneumoniae*. Utilizing a combination of WGM and  
44 WGS, we also present here the first longitudinal genomic characterization of the highly dynamic  
45 carbapenem-resistant ST383 *K. pneumoniae* clone that is rapidly gaining importance in Europe.

## 46 INTRODUCTION

47 The spread of multidrug-resistant *K. pneumoniae* strains in hospitals constitutes a pressing global  
48 health problem. The increasing prevalence of plasmid-encoded carbapenem-hydrolysing enzymes  
49 in *K. pneumoniae* is of particular concern due to their ability to hydrolyse almost all  $\beta$ -lactam  
50 antibiotics, as well as their genetic association with transferable multidrug resistance.<sup>1-3</sup> Infections  
51 due to carbapenem-resistant *K. pneumoniae* are not only difficult to treat due to limited therapeutic  
52 options, but such clones could potentially cause hospital epidemics if not promptly detected and  
53 contained.<sup>4</sup>

54 Molecular typing techniques are effective surveillance tools to monitor the dynamics of multidrug-  
55 resistant clones circulating in hospitals during non-outbreak situations and to detect early signs of  
56 an outbreak. Currently used techniques are based on amplification of marker genes followed by  
57 sequencing (MLST), or targeting entire genomes by PFGE or by whole genome mapping (WGM),  
58 with the restriction fragments analysed on a gel or in a microfluidic device, respectively. Of the  
59 three techniques, MLST is most commonly utilized for bacteria strain typing. While it is highly  
60 reproducible and relatively inexpensive, the resolution achieved by clustering strains based on  
61 sequenced segments of seven or more housekeeping genes is not high enough to study inter- and  
62 intra-clonal genetic diversity. Compared to PFGE, WGM has the advantage of being less labour  
63 intensive and, importantly, allowing inter-lab reproducibility and comparison of results that has  
64 been a major shortcoming of PFGE typing. WGM is also far less technologically challenging than  
65 whole genome sequencing (WGS) and does not require bioinformatics expertise. Furthermore,  
66 results can be generated on the same day with WGM that offers a distinct advantage for  
67 microbiology laboratories undertaking outbreak investigations. Notwithstanding instrument costs,  
68 the cost of running a single strain for PFGE < WGM  $\leq$  WGS. Also with WGM, the genetic  
69 content of the detected variable genome regions can be extracted and identified by utilizing the  
70 vast number of publicly available whole genome sequences. These can be utilized to develop *in*

71 *silico* restriction maps using the same enzymes as used for experimentally-generated WGMs,  
72 allowing comparison of restriction patterns and eventual identification of the genetic content of the  
73 variable regions in the strains of interest.<sup>5</sup>

74 In this study, we demonstrate the utility of WGM in conjunction with WGS for typing,  
75 characterizing, and dissecting the genomic features of carbapenem-resistant *K. pneumoniae*  
76 isolated at the Tzaneio General (TG) hospital, Piraeus, Greece. Carbapenem-resistant *K.*  
77 *pneumoniae* producing VIM-type metallo- $\beta$ -lactamases have been endemic in Greek hospitals  
78 since the early 2000s.<sup>6</sup> Many strains with VIM-1-producing *K. pneumoniae* have also been  
79 described.<sup>7</sup> From 2007, KPC-type carbapenemases became prevalent and even caused outbreaks,<sup>8</sup>  
80 <sup>9</sup> followed by emergence of strains coproducing KPC and VIM.<sup>10</sup> We studied VIM- and KPC-  
81 +VIM-producing *K. pneumoniae* isolated from colonized or infected patients during 2010-2013 at  
82 the TG hospital.

## 83 MATERIALS AND METHODS

### 84 *Strain collection*

85 Twelve *K. pneumoniae* (TGH1-TGH12), harbouring *bla*<sub>VIM</sub> and/or *bla*<sub>KPC</sub>, and isolated from  
86 patients admitted to the intensive care unit (n=8) or surgical ward (n=4) at the TG hospital during  
87 2010-2013 were studied. Clinical data and strain characteristics are outlined in Table 1.

### 88 *Antimicrobial resistance profiling*

89 All 12 strains were screened for resistance to 17 antibiotics, including  $\beta$ -lactams with and without  
90  $\beta$ -lactamase inhibitors, by disk diffusion (Table 1). MICs of carbapenems (ertapenem, imipenem  
91 and meropenem) were determined by Etest (bioMérieux Inc., Durham, NC), and results  
92 interpreted according to CLSI cut-offs.<sup>11</sup> Strains were screened for presence of extended-spectrum  
93  $\beta$ -lactamase (ESBL) and carbapenemase genes by PCR and Sanger sequencing as described  
94 previously.<sup>12-14</sup>

### 95 *MLST and PFGE*

96 MLST was performed as described previously for seven marker genes (*gapA*, *infB*, *mdh*, *pgi*,  
97 *phoE*, *rpoB*, *tonB*),<sup>15</sup> and sequence types were assigned using the Institute Pasteur database  
98 ([www.pasteur.fr/mlst](http://www.pasteur.fr/mlst)). PFGE was performed as follows. Briefly, cells from an overnight blood  
99 agar culture were washed, adjusted to a density of 1.0 OD at 600nm in EC lysis buffer (100 mM  
100 EDTA, 5M NaCl, 0.5% Brij-58, 0.2% deoxycholate, 10% N-laurylsarcosine, 6 mM Tris-HCl pH  
101 7.6), and after centrifugation, resuspended into 200 $\mu$ L EC lysis buffer with 10  $\mu$ L proteinase K  
102 (20mg/mL). Cell suspension was mixed with equal volume of 1.0% (w/v) SeaKem Gold Agarose  
103 (Westburg) to form plugs. These were incubated in 2 mL of EC lysis buffer and 10  $\mu$ L of  
104 proteinase K (20 mg/mL) for 2h at 55°C. The plugs were washed five times at 55°C for 15 min  
105 with sterile water, and digested overnight at 37°C with 50 U of *XbaI* (Life Technologies). Plug  
106 slices were placed on the well comb, and tempered agarose was poured in the gel mould. The gel

107 was run at 6.0 V/cm with an initial switch time of 5 s to a final switch time of 35 s at 14°C in 0.5×  
108 TBE (Tris-borate-EDTA) running buffer for 24 h. DNA band profiles were stained with ethidium  
109 bromide, and visualized and digitized by the Quantity One documentation system (Bio-Rad).  
110 Conversion, normalization and analysis of patterns was carried out using GelCompar software  
111 version 4.0 (Applied Maths, Kortrijk, Belgium) and pattern analyses were performed as described.

112 <sup>16</sup>

### 113 *WGM*

114 The complete genomes of all 12 strains were mapped employing the Argus<sup>®</sup> Whole Genome  
115 Mapping System (Opgen Inc, Gaithersburg, USA). DNA extraction, DNA quality control, DNA  
116 restriction using *AflIII*, and loading on a MapCard were done according to manufacturer's  
117 protocols. Briefly, *K. pneumoniae* colonies grown overnight at 37°C on Mueller-Hinton agar  
118 plates were immobilized in agarose plugs (as described for the PFGE protocol) and subjected to  
119 in-plug gentle lysis, followed by thoroughly washing plugs in TE buffer at 42°C and enzymatic  
120 treatment with β-agarase (New England Biolabs Inc, Ipswich, USA). For WGM, dilutions were  
121 prepared with dilution buffer, and DNA was checked for quality and presence of high molecular  
122 weight DNA molecules (Argus<sup>®</sup> QCard kit, Opgen) and subsequently loaded on the MapCard  
123 (Argus<sup>®</sup> MapCard II kit, Opgen, Inc). *De novo* assembly of restricted DNA fragments was  
124 performed using MapManager software (Opgen). For editing, maps were adjusted in orientation  
125 and in their replication point employing an *in silico* map generated from *K. pneumoniae* KPNIH31  
126 (accession number CP009876.1) using built-in function with default parameters in MapSolver  
127 (Opgen Inc.). All WGMs were analysed by filtering out fragment sizes smaller than 5 kb from the  
128 analysis and using three different set of parameters that allowed clustering, sub-clustering, and  
129 discrepant analysis. Firstly, pattern search was performed with a relative tolerance of 5%, an  
130 absolute tolerance of 2000 (bp) with 1 mismatch and secondary criteria with most identical  
131 matches, and a similarity co-efficient set at 95% was utilised. Secondly, relative tolerance of 1%,

132 absolute tolerance of 1000 bp, pattern length search with 8 fragments to generate a dendrogram  
133 with most identical matches, and a similarity co-efficient of 99% was utilised. Thirdly, the same  
134 parameters as the second analysis were utilised, but instead of similarity, we studied the 'absolute  
135 number of unmatched fragments' between two WGMs assigning  $\geq 10$  unmatched fragments as a  
136 cut-off to assign a new cluster. All pattern-search cluster-analysis was performed using  
137 Bionumerics v7.5 (Applied Maths, Kortrijk, Belgium) employing UPGMA, and similarity matrix  
138 of clusters was defined by Cophenetic Correlation Coefficient (CCC).<sup>17</sup>

### 139 *In silico restriction mapping using AflIII*

140 For two strains, TGH8 and TGH10, which were whole genome sequenced (see below), we  
141 performed *in silico* restriction mapping in order to quantify the fragment losses and other  
142 differences observed with experimentally-generated mapping using WGM. Comparison of *in*  
143 *silico* and experimentally-generated maps of the clinical strains was performed using MapSolver  
144 and BioNumerics v7.5.

### 145 *WGS and comparative genome analysis*

146 Two *K. pneumoniae* isolates (TGH8 and TGH10) were whole genome sequenced. Briefly,  
147 genomic DNA was extracted using MasterPure<sup>TM</sup> DNA Purification Kit (Epicentre Technologies  
148 Corp). WGS was performed using Nextera XT DNA Library Preparation Kit followed by  
149 sequencing via 2 X 150 bp paired end sequencing (Illumina Inc.). The sequence reads of strains  
150 were *de novo* assembled using SPAdes,<sup>18</sup> and annotated using Rapid Annotation Subsystem  
151 technology (RAST) online server.<sup>19,20</sup> *De novo* assembled contigs were aligned against  
152 corresponding whole genome maps in MapSolver in order to generate pseudo chromosomes and  
153 also to identify variable regions and genomic content. To precisely localize the site and  
154 characteristics of the genomic change, sequence contigs corresponding to the regions of genome  
155 divergence were further analysed in CLC Genomics Workbench v7.5.1 (CLCbio, Denmark).  
156 Similarity search of variable regions was performed using NCBI BLAST at nucleotide and protein

157 level.<sup>21-23</sup> Integron (In) sorting and analysis was done as follows: *de novo* assembled contigs were  
158 sorted by length and coverage i.e., >1 kb and > 250-fold coverage, the raw reads were extracted  
159 separately, and *de novo* assembled using SPAdes. The reads were mapped again in order to  
160 validate mis-assemblies using CLC Genomics Workbench (CLCbio), and the contigs annotated  
161 and validated using online databases RAC: (Repository of Antibiotic Resistance Cassettes  
162 <http://rac.aihi.mq.edu.au/rac/>) and INTEGRALL.<sup>24,25</sup> Identification and typing of integrative and  
163 conjugative elements (ICEs) was performed using web-based resource ICEberg.<sup>26</sup> Plasmid  
164 sequence analysis was done as follows. Firstly, the contigs were screened for plasmid origin by  
165 using the online tool “Plasmid finder” (<https://cge.cbs.dtu.dk/services/PlasmidFinder/>).<sup>27</sup> Next, the  
166 generated plasmid-specific contigs were used as a reference template and raw reads were mapped.  
167 Lastly, *de novo* assembly was performed on the mapped reads using CLC Genomics Workbench  
168 v7.5.1 (CLCbio, Denmark) with default parameters.

169 **RESULTS**

170 *Phenotypic and genotypic characterization of K. pneumoniae*

171 Twelve of the 11 strains were carbapenem-resistant of which 7 harboured *bla*<sub>KPC-2</sub> and 11 *bla*<sub>VIM-19</sub>  
172 (Table 1). The ST383 strains exhibited five carbapenemase/ESBL combinations: 1) *bla*<sub>VIM-19</sub>,  
173 *bla*<sub>KPC-2</sub>, and *bla*<sub>CTX-M-15</sub> (TGH1, TGH6, TGH8, TGH9), 2) *bla*<sub>VIM-19</sub>, and *bla*<sub>KPC-2</sub> (TGH2, TGH4,  
174 and TGH5), 3) *bla*<sub>VIM-19</sub>, and *bla*<sub>CTX-M-15</sub> (TGH3), 4) *bla*<sub>CTX-M-15</sub> (TGH7) and 5) *bla*<sub>VIM-19</sub> (TGH10,  
175 TGH11 and TGH12) (Table 1).

176 *Genetic diversification within K. pneumoniae ST383 identified by WGM*

177 Strains TGH1-TGH12 belonged to ST383 and were divided into 3 PFGE types based on a  $\geq 7$ -  
178 band difference. Subtypes were delineated based on a  $\geq 3$ -band difference between profiles  
179 belonging to the same PFGE type (Figure 1). Utilizing a similarity co-efficient cut-off of 95% and  
180 TGH1, the oldest strain in our collection, as the reference map, WGMs of all 12 ST383 strains  
181 were found to form 1 cluster (Figure 2). TGH8 and TGH9 showed maximum dissimilarity (4.7%)  
182 compared to the other 10 strains (Figure 2). Differences between strains were mainly due to  
183 presence of mobile elements such as ICEs, prophages, and transposons. To add further granularity  
184 to our data and observe sub-clusters, we analysed the WGMs using more stringent parameters  
185 (Figure 3A and B). Figure 3A shows clustering based on a similarity co-efficient of 99% and  
186 Figure 3B using a diversity co-efficient (no. of unmatched fragments). Both parameters showed  
187 similar (sub) clustering of WGMs, identifying two clusters, C1 and C2, and two singletons, C3  
188 and C4 (Figure 3B), with C1 and C2 each divided into two sub clusters and a singleton (Figure  
189 3B). In this analysis, TGH9 was found to be the most dissimilar strain showing only 77.4%  
190 similarity or a 124-unmatched fragment difference with the rest of the WGMs (Figure 3A and B).  
191 Insertions in TGH8 and TGH11, identified by WGM analysis, accounted for  $\sim 1.8\%$  and  $\sim 1.2\%$   
192 genomic expansion (Figure 3A), respectively, compared to the other ST383 strains studied here.

193 *Comparison of discriminatory power and congruence between WGM and PFGE*

194 We utilized the adjusted Wallace co-efficient to compare partitions, and the Simpson's diversity  
195 index (SDI) to compare the discriminatory power of WGM and PFGE.<sup>28</sup> As all strains studied here  
196 belonged to one ST type (ST383), no. of partitions achieved with MLST was 1 and hence was not  
197 included in this analyses. Based on the parameter 'no. of unmatched fragments'  $\geq 10$  (or distance  
198 co-efficient) (Figure 3B), we obtained 8 (sub) clusters with WGM that were compared to the  
199 corresponding 3 PFGE types ( $\geq 7$ -band difference) and 8 subtypes ( $\geq 3$ -band difference). Based on  
200 a  $\geq 3$ -band difference between PFGE profiles, no significant difference was observed in the SDI of  
201 WGM (0.94, Jackknife pseudo-values CI: 0.883-0.996) and PFGE (0.93, Jackknife pseudo-values  
202 CI: 0.828-1.000) ( $p = 0.649$ ). The adjusted Wallace co-efficient was also similar for PFGE (0.36,  
203 95% CI: 0.000-0.816,  $\geq 3$ -band difference) and WGM (0.46, 95% CI: 0.076-0.842). However,  
204 discriminatory power of WGM was significantly higher (SDI: 0.94, Jackknife pseudo-values CI:  
205 0.883-0.996) than PFGE based on a  $\geq 7$ -band difference (SDI: 0.53, Jackknife pseudo-values CI:  
206 0.212-0.849) ( $p = 0.007$ ).

207 *Comparing experimentally derived WGM with in-silico restriction mapping using AflIII*

208 In order to assess the reliability and accuracy of the experimentally derived WGMs, we compared  
209 these with *in silico* AflIII restriction maps generated from the whole genome sequencing data of  
210 TGH8 and TGH10 (Figure 4A). AflIII, the manufacturer recommended and optimized enzyme for  
211 *K. pneumoniae* produces 442 (TGH8) and 437 (TGH10) fragments ranging from 78 kb-14 nt.  
212 After removal of the  $< 5$  kb fragment differences, we observed a similarity co-efficient of 80-84%  
213 between the experimental and *in silico* maps (Figure 4A). A similar comparison between PFGE  
214 and XbaI *in silico* restriction mapping was not possible because of the basic difference in map  
215 generation; the former being molecular size based fragmentation and the latter an ordered genome  
216 map. Nonetheless, XbaI *in silico* restriction mapping of TGH8 and TGH10 produced  
217 approximately 45 and 37 fragments respectively (data not shown), while their respective PFGE

218 profiles showed 17 and 15 fragments, respectively, with the < 36 kb fragments lost to follow-up  
219 on PFGE gels (Figure 1).  
220 Comparison of TGH8 experimental and *in silico* maps showed that there were missing restriction  
221 cuts in the former (Figure 4B). The TGH8 *in silico* map generated a total of 442 *AfIII*-restricted  
222 fragments of which 284 were >5 kb, while the experimental map showed a total of 386 fragments  
223 of which 278 were > 5 kb. Similarly, the TGH10 *in silico* map generated a total of 437 *AfIII*-  
224 restricted fragments of which 282 were >5 kb, while the experimental map showed a total of 385  
225 fragments of which 278 were > 5 kb.

### 226 *Intra-cluster comparison of ST383 whole genome maps*

227 Compared to the other ST383 maps, TGH11 and TGH8 showed two unique insertions of ~31 kb  
228 and ~110 kb, respectively (Figure 2). These genomic insertions were unique in our mapped  
229 strains as deduced from comparative analysis of TGH8 and TGH11 maps with *in silico* maps  
230 generated from six previously sequenced *K. pneumoniae* available on NCBI (data not shown). By  
231 aligning the pseudo chromosomes of TGH8 and TGH10 to their corresponding WGMs, it was  
232 possible to pinpoint the sequence region harbouring the insertion in TGH8. The TGH8 insertion  
233 (from 773,512, to 884,869 kb) was identified as 99% homologous to a region present in *Proteus*  
234 *mirabilis* strain HI4320 (2,793,662 to 2,886,224 kb, accession number: AM942759). In TGH8, the  
235 ~110 kb genomic insertion lies in a region of high plasticity as evidenced by presence of flanking  
236 phage and mobile element remnants such as genes encoding phage capsids, phage-associated  
237 hypothetical proteins as well as transposases. Our search of the ~110 kb insertion against the  
238 ICEberg database identified an unclassified ~94 kb *ICEPm1* element, which harbours genes  
239 encoding a putative signal transducer/ampG/MFS, and virulence-associated genes such as F17  
240 fimbrial protein precursor, iron acquisition yersiniabactin synthesis enzyme, soluble lytic murine  
241 transglycosylase, type IV secretory pathway VirD4/B4, and interestingly, a lipid A export ATP-  
242 binding protein/MsbA. Similar searches for the ~ 31 kb insertion in TGH11 did not identify any

243 pathogenic or virulence-related determinants in this region but rather genes encoding for glucan  
244 biosynthesis protein D precursor, permeases of drug/metabolite transporter (DMT), tellurite  
245 resistance proteins (TehA/TehB), benzyl alcohol dehydrogenase, and an uncharacterized  
246 membrane lipoprotein (data not shown).

247 *Analysis of integrons harbouring bla<sub>VIM</sub> variants*

248 Integron analysis of our sequenced strains (TGH8 and TGH10) showed that *bla<sub>VIM-19</sub>* in both  
249 TGH8 and TGH10 was carried on the class 1 integron, *In4863*, which showed 99% nucleotide  
250 level similarity between TGH8 and TGH10 (Figure 5). However, in contrast to the previously  
251 sequenced *In4863* (accession number KF894700), the element in TGH8 and TGH10 harboured a  
252 variant promoter (PcW-TGN-10),<sup>29</sup> showing polymorphism at the 2<sup>nd</sup> base of the -35 sequence  
253 (TT/GACA). In addition, Int1 also showed two predicted amino acid changes (Pro32Arg and  
254 Asn39His) compared to the published *In4863* sequence (Figure 5).

255 *In silico* analysis of plasmid specific contigs using Plasmid finder and comparative sequence  
256 analysis showed that *bla<sub>KPC-2</sub>*, *bla<sub>CTX-M</sub>* and *bla<sub>VIM-19</sub>* were might be carried on three different  
257 plasmids (IncFII(K), IncFIB and IncA/C2, respectively) in TGH8.

258 **DISCUSSION**

259 In this study, we utilized a collection of carbapenem-resistant *K. pneumoniae* isolated during  
260 2010-2013 at the TG hospital, Greece in order to compare currently utilised gene- and genome-  
261 based typing methods as well as to better understand the molecular epidemiology of carbapenem-  
262 resistant *K. pneumoniae* at TGH.

263 MLST assigned all strains studied here to ST383. In concordance, a cut-off of 95% similarity co-  
264 efficient also assigned all WGMs to a single cluster. To allow comparisons with PFGE, which  
265 assigned the ST383 to 3 types based on a  $\geq 7$ -band difference and to 8 subtypes based on a  $\geq 3$   
266 band difference, we utilized a ' $\geq 10$  unmatched fragment' criteria to assign WGM clusters.  
267 Compared to a  $\geq 7$ -band difference in PFGE profiles, WGM showed a significantly higher  
268 discriminatory power while a 3- band difference criteria showed a similar SDI for PFGE and  
269 WGM. Different restriction enzymes had to be employed for these methods; *AfIII* is the  
270 manufacturer recommended enzyme for whole genome mapping of *K. pneumoniae*, however  
271 fragment sizes with this enzyme range from 78 kb to 14 nt. As a large number of *AfIII*-generated  
272 fragments fall below the resolution of PFGE gels (<36 kb fragments in our hands, Figure 1), we  
273 utilized *XbaI* for the latter method. *In silico* mapping of TGH8 with *AfIII* and *XbaI* generated 442  
274 and 45 (556 kb to 197 nt) fragments, respectively. However, on-gel *XbaI* PFGE profiles consisted  
275 of, on average, 14 bands. Comparison of experimental and *in silico* maps also highlighted the  
276 challenges WGM faces for scoring of small fragments. Of the 56 and 52 missing fragments in the  
277 TGH8 and TGH10 experimental WGMs compared to their *in silico* maps, 50 and 48 (11% for  
278 both) were < 5 kb, respectively. This corresponds to a small fragment loss of 32%. In contrast,  
279 fragment loss rate of > 5 kb fragments was only 1.4-2.1% for both TGH8 and TGH10 WGMs.  
280 Despite lack of evident differences in discriminatory power between PFGE and WGM, which  
281 might be due to the fact that the number of strains analysed here were limited and were closely  
282 related, a major advantage of WGM is that the technique produces an ordered genome map that

283 allows comparison to previously sequenced genomes for identifying larger (> 5 kb)  
284 insertions/deletions. For instance, prior to sequencing, we had already identified the insertion  
285 observed in the WGM of TGH8 as an *ICEPm1* element by comparing with *in silico* maps  
286 generated from six previously sequenced *K. pneumoniae* available on NCBI. This element has  
287 been shown to originate from *P. mirabilis*, and is also highly conserved in other uropathogens  
288 such as *Providencia stuartii* and *Morganella morganii*.<sup>30</sup> Interestingly, the *ICEPm1* element is  
289 known to transfer in a site-specific manner, using phenylalanine tRNA genes as an integration site,  
290<sup>31</sup> and may contribute to fine tuning and adaptation of *K. pneumoniae* towards preferred infection  
291 or colonization pathways.<sup>32</sup>

292 ST383 is a recently described clone that was first detected in Greek hospitals during 2009-2010.<sup>33</sup>  
293 Majority of the ST383 strains circulating in various Greek hospitals during 2009-2010 reportedly  
294 co-harboured *bla*<sub>VIM-4</sub>, *bla*<sub>KPC-2</sub> and *bla*<sub>CMY-4</sub> β-lactamases.<sup>33</sup> Recent studies of 1-3 isolates of  
295 ST383 *K. pneumoniae* recovered during 2008-2010 have also reported presence of *bla*<sub>VIM-19</sub> in this  
296 ST type.<sup>34, 35</sup> ST383 strains isolated at TGH in 2010-11 harboured the *bla*<sub>VIM-19</sub>, *bla*<sub>KPC-2</sub> and  
297 *bla*<sub>CTX-M-15</sub> plasmids in various combinations, while one isolate that was carbapenem-susceptible  
298 did not harbour a carbapenemase. On the other hand, strains isolated in 2013 (TGH10, TGH11 and  
299 TGH12) harboured only *bla*<sub>VIM-19</sub>. These data underscore the remarkable plasticity of ST383 in  
300 terms of the accessory genome. Subject to the limited high-level MIC resolution allowed by Etest,  
301 carbapenem resistance remained high in the TGH10, TGH11 and TGH12 isolates despite loss of  
302 *bla*<sub>KPC-2</sub>, and potentiates the possibility that plasmid loss might have benefitted the ST383 strains  
303 in terms of fitness and transmissibility.

304 The *bla*<sub>VIM-19</sub> carbapenemase is also a new metallo-β-lactamase (MBL) gene variant isolated in  
305 Algiers in 2009.<sup>36</sup> It is known to be derived from *bla*<sub>VIM-1</sub>, differing from the former by two  
306 substitutions: Ser228Arg and Asn215Lys,<sup>36</sup> which confer higher resistance to the carbapenems in  
307 comparison to *bla*<sub>VIM-1</sub>.<sup>37</sup> Accordingly, all *bla*<sub>VIM-19</sub> harbouring ST383 in this study, irrespective of

308 the presence of *bla*<sub>KPC-2</sub>, showed high-level resistance to meropenem, imipenem and ertapenem.  
309 Pournaras *et al.* have reported presence of *bla*<sub>VIM-19</sub> in a *K. pneumoniae* clinical strain co-  
310 producing *bla*<sub>KPC-2</sub> carbapenemase, *bla*<sub>CMY-2</sub> cephalosporinase and *bla*<sub>CTX-M-15</sub> extended-spectrum  
311  $\beta$ -lactamase.<sup>38</sup> They found the *bla*<sub>VIM-19</sub> gene to be associated with a new class 1 integron with a  
312 structure similar to that carrying the close variant gene *bla*<sub>VIM-4</sub> in an *Enterobacter cloacae* isolate  
313 from Greece.<sup>38</sup> The *bla*<sub>VIM-19</sub> gene cassette was located downstream of the *attI1* recombination  
314 site, followed by an *aacA6* cassette, a *dfrA1* cassette, an *aadA1* cassette and the 3'-CS, containing  
315 *qacEA1* and *sull*.<sup>38</sup> Another study has shown *bla*<sub>VIM-19</sub> to be harboured on *In4863*.<sup>35</sup> In our *In4863*-  
316 like element, the *bla*<sub>VIM-19</sub> gene cassette was located downstream of the *attI1* recombination site,  
317 followed by an *aacA6* cassette, a *dfrA1b/15* cassette, an *aad $\Delta$ A1* cassette and the  $\Delta$ *smr2/sugE*  
318 (Quaternary ammonium compound-resistance protein) truncated by *ISPa21*. Furthermore, the  
319 *In4863*-like element differed from the previously described *In4863* by two (predicted) amino acid  
320 substitutions in the integrase and one nucleotide change at the 2<sup>nd</sup> position (T>G) in the integron  
321 promoter sequence. Interestingly, a recent study showed that these changes result in increased  
322 integrase activity and a concomitant decrease in promoter strength,<sup>29</sup> which hypothetically would  
323 increase the frequency of recombination events and acquisition of novel gene cassettes by the  
324 *In4863*-like element under antibiotic pressure. Also, the proximity of the gene cassette to the  
325 integron promoter influences its expression; closer the gene cassette to the promoter higher the  
326 expression. An *in vitro* study analysed the impact of chloramphenicol pressure on gene cassette  
327 rearrangements in a class 1 integron harbouring the chloramphenicol-resistance encoding *catB9*  
328 gene, and found a wide variety of rearrangements under chloramphenicol pressure all leading to  
329 increased proximity of *catB9* to the integron promoter.<sup>39</sup> Remarkably, all known MBL gene  
330 cassettes, including those harbouring *bla*<sub>VIM-19</sub>, have been found to be consistently placed next to  
331 the integron's promoter.<sup>35, 40</sup> Sustained carbapenem use and selection pressure in hospital

332 environments are likely responsible for maintenance of MBL gene cassettes in this priority  
333 position.

334 To conclude, this study demonstrated the application of whole genome mapping to understanding  
335 the epidemiology of hospital-associated *K. pneumoniae*. Additionally, a combination of whole  
336 genome mapping and sequencing provided novel insights on the genomic features of the multi-  
337 drug resistant ST383 *K. pneumoniae* clone that is rapidly gaining importance in terms of  
338 prevalence and clinical significance in Europe.

339 **Acknowledgements**

340 The authors thank Sabine Chapelle for providing excellent technical assistance.

341 **Funding**

342 This work was partly financially supported by EU grants, RGNOSIS (Resistance in Gram-  
343 Negative Organisms: Studying Intervention Strategies, FP7 HEALTH.2011.2.3.1-3, #282512),  
344 and PREPARE (Platform foR European Preparedness Against (Re-)emerging Epidemics, EU-FP7,  
345 # 602525), and by Opgen Inc., Gaithersburg, USA in the framework of the European Public  
346 Health Initiative (EUPHi). B.B.X. is supported by University of Antwerp Research Funds (BOF-  
347 DOCPRO 2012-27450).

348

349 **Transparency declarations**

350 The authors declare no transparency declarations

351 **Genbank depositions**

352 The accession numbers for the integron (*In4863*-like) and whole genome sequences deposited in  
353 Genbank are as follows; *In4863*-like (KT820212), TGH8 (CP012743) and TGH10 (CP012744).

354 **References**

- 355 1. Mathers AJ, Cox HL, Kitchel B et al. Molecular Dissection of an Outbreak of Carbapenem-  
356 Resistant Enterobacteriaceae Reveals Intergenous KPC Carbapenemase Transmission through a  
357 Promiscuous Plasmid. *mBio* 2011; **2**: e00204-11.
- 358 2. Stapleton PD, Shannon KP, French GL. Carbapenem resistance in *Escherichia coli* associated  
359 with plasmid-determined CMY-4 beta-lactamase production and loss of an outer membrane  
360 protein. *Antimicrobial agents and chemotherapy* 1999; **43**: 1206-10.
- 361 3. Goren MG, Carmeli Y, Schwaber MJ et al. Transfer of carbapenem-resistant plasmid from  
362 *Klebsiella pneumoniae* ST258 to *Escherichia coli* in patient. *Emerging infectious diseases* 2010;  
363 **16**: 1014-7.
- 364 4. Saidel-Odes L, Borer A. Limiting and controlling carbapenem-resistant *Klebsiella pneumoniae*.  
365 *Infection and drug resistance* 2013; **7**: 9-14.
- 366 5. Miller JM. Whole-genome mapping: a new paradigm in strain-typing technology. *J Clin*  
367 *Microbiol* 2013; **51**: 1066-70.
- 368 6. Miyakis S, Pefanis A, Tsakris A. The Challenges of Antimicrobial Drug Resistance in Greece.  
369 *Clinical Infectious Diseases* 2011; **53**: 177-84.
- 370 7. Poulou A, Spanakis N, Pournaras S et al. Recurrent healthcare-associated community-onset  
371 infections due to *Klebsiella pneumoniae* producing VIM-1 metallo- $\beta$ -lactamase. *Journal of*  
372 *Antimicrobial Chemotherapy* 2010; **65**: 2538-42.
- 373 8. Pournaras S, Protonotariou E, Voulgari E et al. Clonal spread of KPC-2 carbapenemase-  
374 producing *Klebsiella pneumoniae* strains in Greece. *Journal of Antimicrobial Chemotherapy* 2009;  
375 **64**: 348-52.
- 376 9. Maltezou HC, Giakkoupi P, Maragos A et al. Outbreak of infections due to KPC-2-producing  
377 *Klebsiella pneumoniae* in a hospital in Crete (Greece). *Journal of Infection* 2009; **58**: 213-9.
- 378 10. Giakkoupi P, Pappa O, Polemis M et al. Emerging *Klebsiella pneumoniae* Isolates  
379 Coproducing KPC-2 and VIM-1 Carbapenemases. *Antimicrobial agents and chemotherapy* 2009;  
380 **53**: 4048-50.
- 381 11. Clinical and Laboratory Standards Institute. *Performance Standards for Antimicrobial*  
382 *Susceptibility Testing: 24th Informational Supplement M100-S24*. CLSI, Wayne, PA, USA, 2014.
- 383 12. Monstein HJ, Östholm-Balkhed Å, Nilsson MV et al. Multiplex PCR amplification assay for  
384 the detection of blaSHV, blaTEM and blaCTX-M genes in Enterobacteriaceae. *APMIS* 2007; **115**:  
385 1400-8.
- 386 13. Poirel L, Walsh TR, Cuvillier V et al. Multiplex PCR for detection of acquired carbapenemase  
387 genes. *Diagnostic microbiology and infectious disease* 2011; **70**: 119-23.
- 388 14. Mabilat C, Goussard S, Sougakoff W et al. Direct sequencing of the amplified structural gene  
389 and promoter for the extended-broad-spectrum beta-lactamase TEM-9 (RHH-1) of *Klebsiella*  
390 *pneumoniae*. *Plasmid* 1990; **23**: 27-34.
- 391 15. Diancourt L, Passet V, Verhoef J et al. Multilocus sequence typing of *Klebsiella pneumoniae*  
392 nosocomial isolates. *J Clin Microbiol* 2005; **43**: 4178-82.
- 393 16. Tenover FC, Arbeit RD, Goering RV et al. Interpreting chromosomal DNA restriction patterns  
394 produced by pulsed-field gel electrophoresis: criteria for bacterial strain typing. *J Clin Microbiol*  
395 1995; **33**: 2233-9.
- 396 17. Boopathi NM, & SpringerLink (Online service). . *Genetic mapping and marker assisted*  
397 *selection: Basics, practice and benefits*: Springer India, 2013.
- 398 18. Bankevich A, Nurk S, Antipov D et al. SPAdes: a new genome assembly algorithm and its  
399 applications to single-cell sequencing. *Journal of computational biology : a journal of*  
400 *computational molecular cell biology* 2012; **19**: 455-77.
- 401 19. Aziz RK, Bartels D, Best AA et al. The RAST Server: Rapid Annotations using Subsystems  
402 Technology. *BMC Genomics* 2008; **9**: 75-.

- 403 20. Overbeek R, Olson R, Pusch GD et al. The SEED and the Rapid Annotation of microbial  
404 genomes using Subsystems Technology (RAST). *Nucleic Acids Research* 2014; **42**: D206-D14.
- 405 21. Altschul SF, Gish W, Miller W et al. Basic local alignment search tool. *Journal of molecular*  
406 *biology* 1990; **215**: 403-10.
- 407 22. States DJ, Gish W. Combined use of sequence similarity and codon bias for coding region  
408 identification. *Journal of computational biology : a journal of computational molecular cell*  
409 *biology* 1994; **1**: 39-50.
- 410 23. Cosentino S, Voldby Larsen M, Møller Aarestrup F et al. PathogenFinder - Distinguishing  
411 Friend from Foe Using Bacterial Whole Genome Sequence Data. *PloS one* 2013; **8**: e77302.
- 412 24. Tsafnat G, Copty J, Partridge SR. RAC: Repository of Antibiotic resistance Cassettes.  
413 *Database* 2011; **2011**.
- 414 25. Moura A, Soares M, Pereira C et al. INTEGRALL: a database and search engine for integrons,  
415 integrases and gene cassettes. *Bioinformatics* 2009; **25**: 1096-8.
- 416 26. Bi DX, Xu Z, Harrison EM et al. ICEberg: a web-based resource for integrative and  
417 conjugative elements found in Bacteria. *Nucleic Acids Research* 2012; **40**: D621-D6.
- 418 27. Carattoli A, Zankari E, García-Fernández A et al. In Silico Detection and Typing of Plasmids  
419 using PlasmidFinder and Plasmid Multilocus Sequence Typing. *Antimicrobial agents and*  
420 *chemotherapy* 2014; **58**: 3895-903.
- 421 28. Carriço JA, Silva-Costa C, Melo-Cristino J et al. Illustration of a Common Framework for  
422 Relating Multiple Typing Methods by Application to Macrolide-Resistant *Streptococcus*  
423 *pyogenes*. *Journal of Clinical Microbiology* 2006; **44**: 2524-32.
- 424 29. Jové T, Da Re S, Denis F et al. Inverse Correlation between Promoter Strength and Excision  
425 Activity in Class 1 Integrons. *PLoS Genet* 2010; **6**: e1000793.
- 426 30. Flannery EL, Mody L, Mobley HLT. Identification of a Modular Pathogenicity Island That Is  
427 Widespread among Urease-Producing Uropathogens and Shares Features with a Diverse Group of  
428 Mobile Elements. *Infection and Immunity* 2009; **77**: 4887-94.
- 429 31. Flannery EL, Antczak SM, Mobley HLT. Self-Transmissibility of the Integrative and  
430 Conjugative Element ICEPm1 between Clinical Isolates Requires a Functional Integrase,  
431 Relaxase, and Type IV Secretion System. *J Bacteriol* 2011; **193**: 4104-12.
- 432 32. Chen N, Ou H-Y, van Aartsen J et al. The pheV Phenylalanine tRNA Gene in  
433 *Klebsiella pneumoniae* Clinical Isolates Is an Integration Hotspot for Possible Niche-Adaptation  
434 Genomic Islands. *Curr Microbiol* 2010; **60**: 210-6.
- 435 33. Papagiannitsis CC, Giakkoupi P, Vatopoulos AC et al. Emergence of *Klebsiella pneumoniae*  
436 of a novel sequence type (ST383) producing VIM-4, KPC-2 and CMY-4 beta-lactamases.  
437 *International journal of antimicrobial agents* 2010; **36**: 573-4.
- 438 34. Samuelsen Ø, Toleman MA, Hasseltvedt V et al. Molecular characterization of VIM-  
439 producing *Klebsiella pneumoniae* from Scandinavia reveals genetic relatedness with international  
440 clonal complexes encoding transferable multidrug resistance. *Clinical Microbiology and Infection*  
441 2011; **17**: 1811-6.
- 442 35. Papagiannitsis CC, Izdebski R, Baraniak A et al. Survey of metallo- $\beta$ -lactamase-producing  
443 Enterobacteriaceae colonizing patients in European ICUs and rehabilitation units, 2008–11.  
444 *Journal of Antimicrobial Chemotherapy* 2015; **70**: 1981-8.
- 445 36. Robin F, Aggoune-Khinache N, Delmas J et al. Novel VIM Metallo- $\beta$ -Lactamase Variant  
446 from Clinical Isolates of Enterobacteriaceae from Algeria. *Antimicrobial agents and*  
447 *chemotherapy* 2010; **54**: 466-70.
- 448 37. Rodriguez-Martinez J-M, Nordmann P, Fortineau N et al. VIM-19, a Metallo- $\beta$ -Lactamase  
449 with Increased Carbapenemase Activity from *Escherichia coli* and *Klebsiella pneumoniae*.  
450 *Antimicrobial agents and chemotherapy* 2010; **54**: 471-6.

- 451 38. Pournaras S, Poulou A, Voulgari E et al. Detection of the new metallo- $\beta$ -lactamase VIM-19  
452 along with KPC-2, CMY-2 and CTX-M-15 in *Klebsiella pneumoniae*. *Journal of Antimicrobial*  
453 *Chemotherapy* 2010; **65**: 1604-7.
- 454 39. Barraud O, Ploy M-C. Diversity of Class 1 Integron Gene Cassette Rearrangements Selected  
455 Under Antibiotic Pressure. *J Bacteriol* 2015.
- 456 40. Zhao W-H, Hu Z-Q. Acquired metallo- $\beta$ -lactamases and their genetic association with class 1  
457 integrons and ISCR elements in Gram-negative bacteria. *Future Microbiology* 2015; **10**: 873-87.  
458  
459  
460

461 **Legends to Figures and Tables**

462 **Figure 1.** PFGE types ( $\geq 7$ -band difference) and subtypes ( $\geq 3$ -band difference) of *K. pneumoniae*  
463 ST383

464  
465 **Figure 2.** Comparison of whole genome maps of ST383 strains. Green shaded areas indicate  
466 identical restriction patterns among the maps and red horizontal marks represent variations. A  
467 similarity co-efficient of 95% was utilised which assigned the strain to a single cluster.

468  
469 **Figure 3.** Comparison of whole genome maps of ST383 strains using a similarity coefficient of  
470 99% **(A)**, and a ' $\geq 10$  unmatched fragments' criterion **(B)**. Both parameters showed similar (sub)  
471 clustering of WGMs, identifying two clusters (C1 and C2) and two singletons (C3 and C4) with  
472 C1 and C2 each divided into two sub clusters and a singleton.

473  
474 **Figure 4.** Comparison of experimental and *in silico* restriction maps using *AflIII* that show  
475 fragment losses ranging from 28 kb to 43 kb in both experimental and *in silico* maps **(A)**.  
476 Comparison of zoomed-in experimental and *in silico* restriction map of TGH8 showing missing  
477 restriction enzyme cuts in the former **(B)**.

478  
479 **Figure 5.** Gene cassette arrangement in Class 1 integrons harboured by ST383 (*In4863*-like) and  
480 Int1 protein alignment. Amino acids boxed in black represent variation in the Int1 protein between  
481 TGH8 and TGH10 ST383 compared to published Class 1 integrases.

**Table 1.** Clinical data and characteristics of strains under study

Strain ID	Clinical information			Molecular typing								Resistance profile											
	Unit	Site of isolation	Isolation date	PFGE*	ST type	WGM Type	<i>bla</i> -genes					MIC by E test			Sensitivity by Disk Diffusion**								
							<i>bla</i> <sub>VIM</sub>	<i>bla</i> <sub>KPC</sub>	<i>bla</i> <sub>CTX-M</sub>	<i>bla</i> <sub>SHV</sub>	<i>bla</i> <sub>TEM</sub>	Meropenem	Ertapenem	Imipenem	Fosfomycin	Cefoxitin	Gentamicin						
TGH1	ICU	Blood	Jan-10	3a	ST383	C1a	VIM-19	KPC-2	CTX-M-15	SHV-1	TEM-1	R	>32	R	>32	R	>32	S	19	R	0	R	0
TGH2	S	Wound Swab	Feb-10	1a	ST383	C2b	VIM-19	KPC-2	-	SHV-1	TEM-1	R	>32	R	>32	R	>32	S	19	R	0	S	21
TGH3	ICU	Urinary Catheter	Apr-10	1b	ST383	C1a	VIM-19	-	CTX-M-15	SHV-1	-	R	>32	R	>32	R	>32	S	19	R	0	R	0
TGH4	S	Urine	May-10	1a	ST383	C2b	VIM-19	KPC-2	-	SHV-1	TEM-1	R	>32	R	>32	R	>32	S	20	R	0	S	21
TGH5	ICU	Blood	May-10	3a	ST383	C1b	VIM-19	KPC-2	-	SHV-1	TEM-1	R	>32	R	>32	R	>32	S	19	R	0	S	22
TGH6	ICU	CVC	Aug-10	1d	ST383	C1b	VIM-19	KPC-2	CTX-M-15	SHV-1	-	R	>32	R	>32	R	>32	S	21	R	0	R	0
TGH7	S	Urine	Nov-10	1c	ST383	C2c	-	-	CTX-M-15	SHV-1	-	S	0.023	S	0,023	S	0.19	S	21	I	15	R	0
TGH8	ICU	CVC	Jun-11	2a	ST383	S3	VIM-19	KPC-2	CTX-M-15	SHV-1	TEM-1	R	>32	R	>32	R	>32	R	0	R	0	R	0
TGH9	ICU	Blood	Aug-11	3b	ST383	S4	VIM-19	KPC-2	CTX-M-15	SHV-1	TEM-1	R	>32	R	>32	R	>32	S	18	R	0	R	0
TGH10	ICU	Wound Swab	Mar-13	1b	ST383	C2a	VIM-19	-	-	SHV-1	-	R	>32	R	>32	R	>32	S	18	R	0	R	0
TGH11	ICU	Rectal	Apr-13	1e	ST383	C1c	VIM-19	-	-	SHV-1	-	R	>32	R	>32	R	>32	S	19	R	0	R	0
TGH12	S	Blood	Apr-13	1b	ST383	C2a	VIM-19	-	-	SHV-1	-	R	>32	R	>32	R	>32	S	19	R	0	R	0

\*To define a PFGE type,  $\geq 7$ -band difference cut-off was utilized. The number of band differences between the subtypes is 1, which indicates that the strains were genetically closely-related.

\*\* All strains were resistant to the following antibiotics by disc diffusion: amoxicillin, piperacillin, amoxicillin-clavulanic acid, piperacillin-tazobactam, cefepime, cefotaxime, ceftazidime, aztreonam, ciprofloxacin, nitrofurantoin, trimethoprim- sulfamethoxazole.

Abbreviations: SS - surgical site, ICU - intensive care unit, CVC - central venous catheter, R – resistant, S - susceptible.

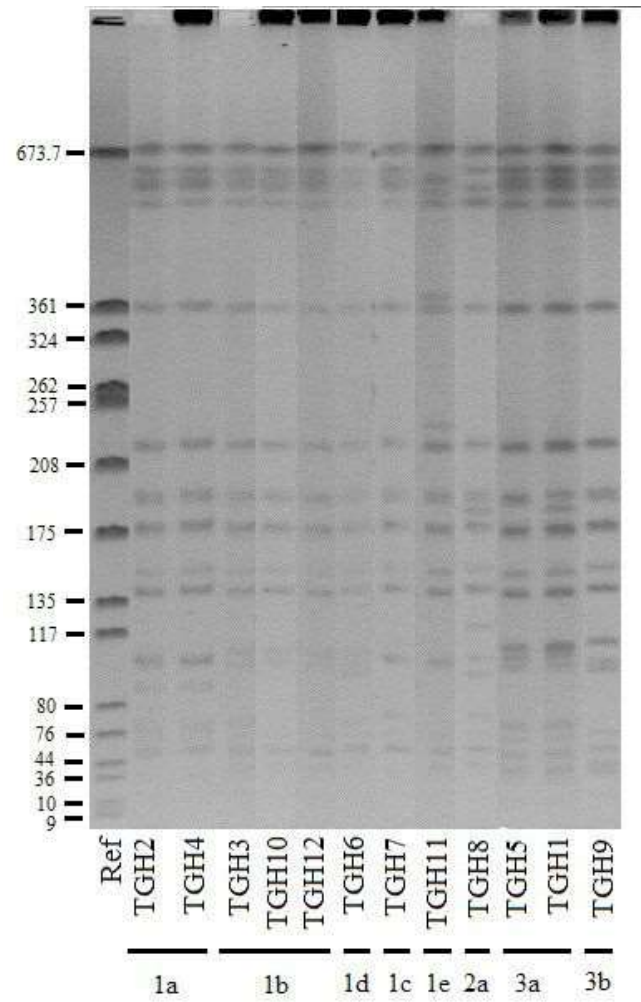


**Figure 1**



**Figure 2**



Figure 3

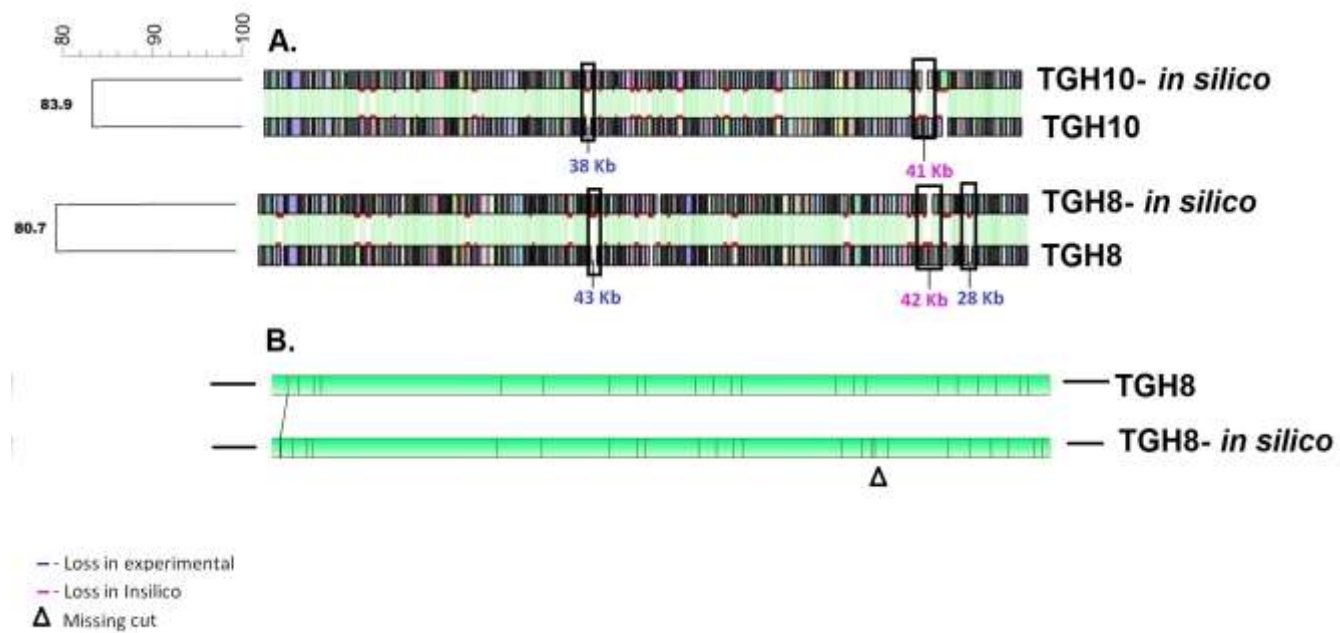


Figure 4

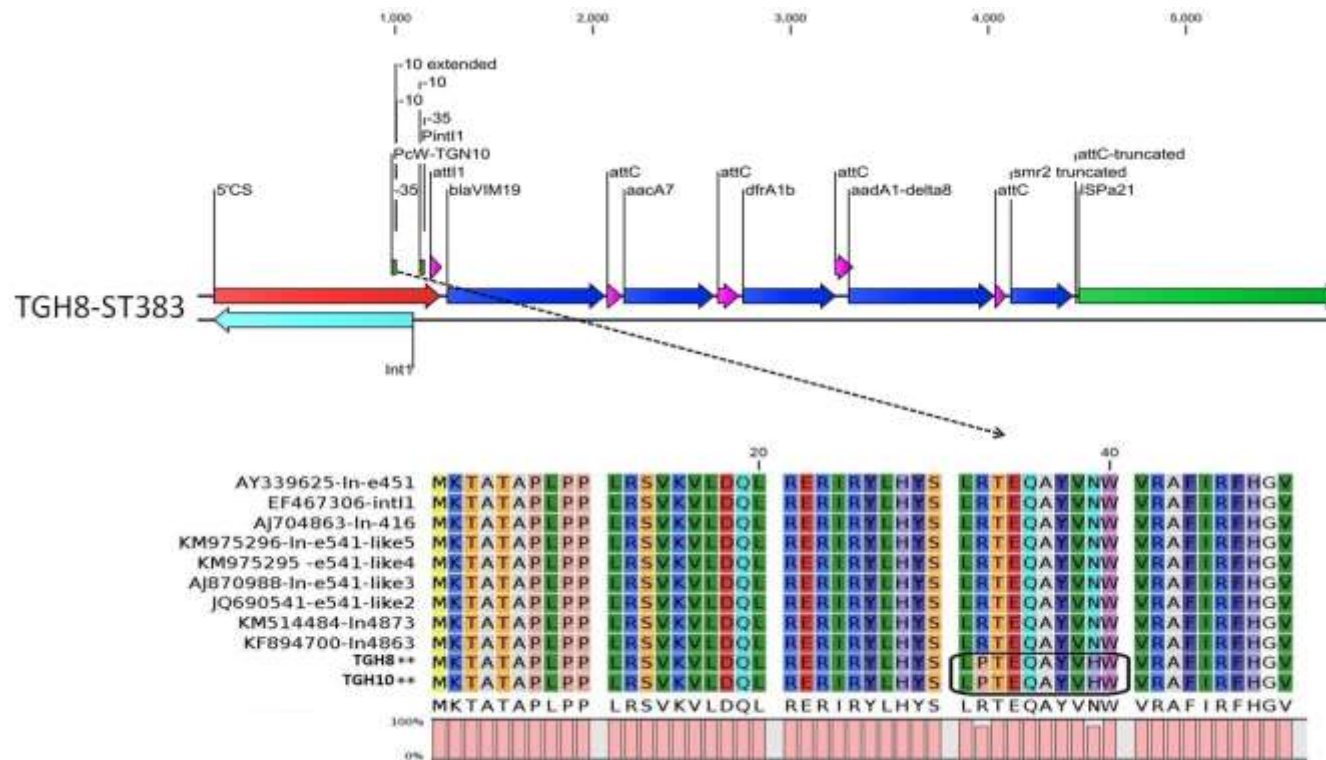


Figure 5